2011 American Control Conference
on O'Farrell Street, San Francisco, CA, USA
June 29 - July 01, 2011

Capacitance Ratio Estimation on a Novel MEMS Tactile Sensor for Elasticity Measurement

Peng Peng, *Student Member*, *IEEE*, and Rajesh Rajamani, *Senior Member*, *IEEE*

***Abstract*—This paper develops a real-time capacitance ratio estimation system for a novel MEMS tactile sensor that can provide elasticity measurement of a variety of target objects. The tactile sensor is developed by this team for in-vivo tissue elasticity measurements and can be installed on a hand-held probe or on minimally invasive surgical instruments. The sensor readout consists of two channels of capacitance values and the ratio of these capacitance values needs to be reliably estimated in real-time. The proposed estimation algorithm utilizes a recursive least squares method with adaptive forgetting factors, which provides reliable elasticity measurement of polymer specimens and quickly detects changes in elasticity. Extensive experimental results are presented.**

I. Introduction

ELASTICTY MEASUREMENT is important in biomedical sensing, robotics, and various industrial applications. For instance, in robotic manipulations, knowledge of elasticity of the targeted object would enable better control of the contact force in a precision grasp [1]. In biomedical applications, in-vivo measurement of tissue elasticity can facilitate doctors to reach a reliable palpation diagnosis [2], to evaluate the health of tissue [3], and to provide tactile perception during a minimally invasive surgery (MIS) [4] .

Although in-vivo measurement of tissue elasticity is essential in physical examination, very few examples of elasticity sensors have been previously developed. A commonly used approach for elasticity measurement is to measure the force-displacement response of the tissue under examination. However, this type of device always includes an actuating element to provide a controlled deformation or force on the tissue, which becomes an obstacle for miniaturization of the device and also increases the fabrication complexity. This approach would become even more challenging in applications within a confined space (e.g. MIS).

A novel tactile sensor has been developed by this team for elasticity measurement [5-7]. This novel approach enables elasticity measurement based on the relative deflection of two sensing diaphragms. These two diaphragms are designed to have different stiffness values. Neither displacement nor applied load needs to be measured during the contact. Further, prototypes of sensors have been fabricated through both a surface micromachining process [5, 6] and a polymer MEMS process [7]. The sizes of the prototype sensors can be fabricated to be of the order of 1mm x1mm.

The prototype sensors are designed to generate capacitance signals for the two sensing elements. The ratio of these two capacitance signals is used to calculate the elasticity property of the targeted object. As a tactile sensor operating in a hand-held mode, however, interference from hand vibration would increase the noise level of the readouts. The real-time identification of the capacitance ratio therefore can be very challenging. In order to provide a reliable estimation of the capacitance ratio, a recursive least square algorithm is developed in this paper to process the two capacitance signals. Further, an adaptive algorithm for choosing forgetting factors is also employed to achieve fast detection of elasticity change, which is an important property during in-vivo tissue characterization. This paper will discuss the design and fabrication of a low cost prototype sensor, design of the identification algorithm, and experimental characterization of the estimation system by measurements on a variety of rubber specimens.

II. Sensor Design and Fabrication

The tactile sensor is composed of two sensing bumps with different stiffness values. As shown in Fig. 1, one of the bumps of the sensor is designed to be harder than the other. Both the bumps are integrated on a solid substrate. During the contact with the targeted object with a stiffness of k_o, the softer bump (k_s) deforms more than its harder counterpart (k_h). Meanwhile, the contact area of the targeted object also undergoes some deflection due to the contact force.

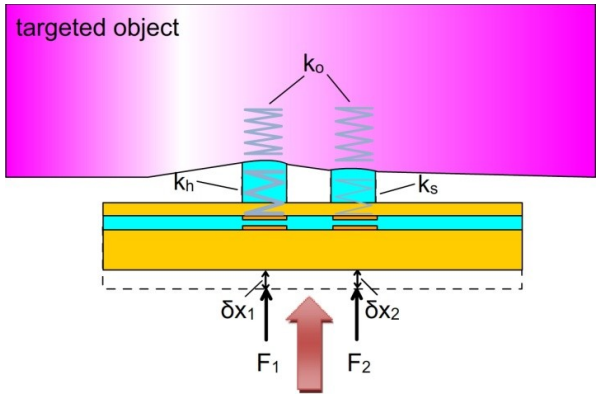

Fig.1. Schematic diagram of the sensing concept.

Manuscript received September 22nd, 2010. Financial support of this work is partly provided by the Minimally Invasive Medical Technologies Center (MIMTeC, www.mimtec.org), a National Science Foundation – Industry – University Cooperative Research Center.

The authors are with the Department of Mechanical Engineering, University of Minnesota, Minneapolis, MN 55455 USA (e-mail: rajamani@me.umn.edu)

Since both sensing elements share a solid substrate, the compatibility condition of the contact can be derived as shown below.

$$\delta x_1 = \delta x_2 \Rightarrow \frac{F_1(k_h + k_o)}{k_h k_o} = \frac{F_2(k_s + k_o)}{k_s k_o} \quad (1)$$

where δx_1 and δx_2 represent the overall displacement of the senor, whereas F_1 and F_2 are contact forces distributed on the two sensing bumps. The stiffness of the targeted object can be therefore calculated from (2)

$$k_o = \frac{(r_F - 1)k_h}{k_h / k_s - r_F} \quad (2)$$

where r_F represents the ratio of the contact force applied on the two bumps (F_1/F_2), while k_h and k_s represent stiffness values of the two bumps, respectively. To precisely measure the contact force on each bump, two force gauges with capacitance readouts are integrated underneath the bumps. The ratio of capacitance readouts $r_c = \delta C_1 / \delta C_2$ can therefore be used to replace the force ratio in (2). Furthermore, a more precise model has been discussed in our previous work [6]. In that model, the targeted object can be roughly modeled as a semi-infinite space when the dimensions of the sensing bumps are much smaller than the object. In this contact scenario, the capacitance ratio r_C can be used as a direct measurement of elasticity (instead of stiffness) of the object. This parameter r_C will be identified using the developed estimation algorithm as described in the next section.

In order to understand how the capacitance readouts are generated, a schematic diagram of the sensor structure is shown in Fig. 2. The capacitors are constituted by a top electrode layer as a common electrode and two separated electrodes on the bottom. An insulator layer is sandwiched between two electrodes as the dielectric. Two bumps are mounted on top of the capacitors serving as the contact interface. The two bumps are designed to have different stiffness values.

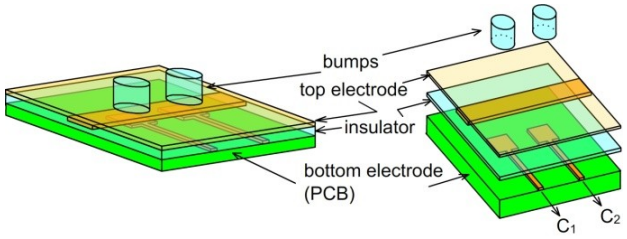

Fig. 2.Schematic diagram of sensor structure.

A brief description of the fabrication process is shown in Fig. 3. As can be seen, the fabrication of the top electrode starts by patterning the copper layer on a polyimide substrate (DuPont™ Pyralux® AC 182500R). To fabricate the bumps, an acrylic mold with concaves for bumps is first made by a computer-controlled driller. Urethane rubber compound (PMC-724, Smooth-On Inc.) is then dripped on the substrate to fill the concaves. The hardness values of this rubber compound are carefully adjusted to Shore 40A and Shore 6A, respectively, thus creating a hard and a soft bump. A blade is used to squeegee the substrate surface to remove the extra rubber compound. These bumps should then be aligned and bonded with the polyimide substrate within half an hour before the rubber curing. After the bonding, the bumps are left for curing overnight and then peeled off from the mold. The final stage is to bond the top and bottom electrode. The bottom electrodes are designed and fabricated using a printed circuit board (PCB) manufacturer. Rubber compound with the hardness of Shore 40A is then poured onto the bottom electrode. Finally, the top electrode and the bottom electrode are aligned and bonded together to complete the sensor fabrication.

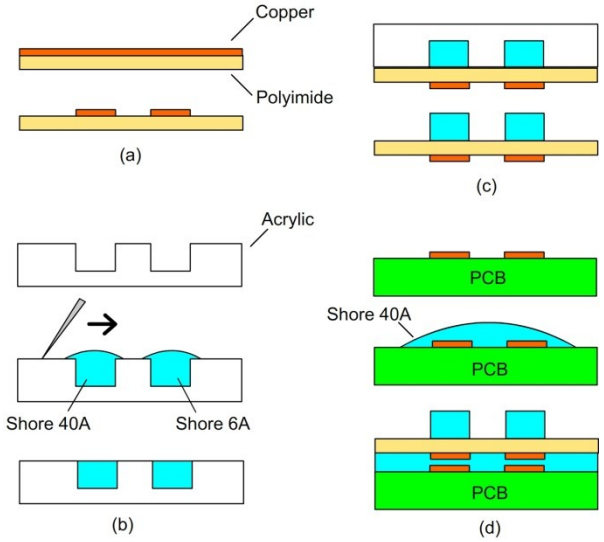

Fig. 3. Fabrication of the tactile sensor: (a) top electrode (b) bumps (c) bonding of top electrode and bumps (d) bonding of top electrode and bottom electrode, completed sensor.

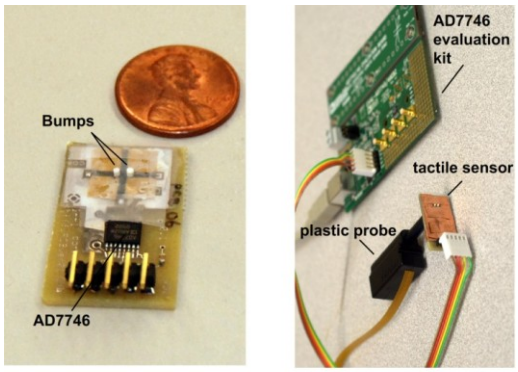

Fig. 4. (a) Fabricated tactile sensor (b) tactile sensor attached on a plastic probe.

In order to generate the capacitance readouts, a capacitance to digital converter (CDC) chip (AD7746, Analog Devices, Inc) is integrated on the PCB board together with the tactile sensor as shown in Fig. 4(a). The capacitance values are converted to digital signals, which are then transmitted to a laptop through an interface AD7746 evaluation kit. Further, to prevent electromagnetic interference (EMI) caused by moving the sensor towards conductors or objects with charge (e.g. tissue), a shielding layer is attached on the sensor

surface. The shielded sensor is finally attached on a plastic probe for operation in a handheld mode as shown in Fig. 4(b).

III. Identification Algorithm Design

The fabricated tactile sensor is tested by pushing against a variety of sorbothane rubber specimens (Part No. 8450K3, McMaster-Carr) as shown in Fig. 5. The Young's moduli of the rubber specimens are listed in Table I. These values of Young's modulus are measured by a rheometer (RMS 800, Rheometrics Scientific). As aforementioned, the sensor readout is composed of two channels of capacitance values, and the ratio (r_c) can be used to represent the elasticity of the targeted rubber sample. However, due to vibrations of the hand holding the sensor probe, a considerable amount of interference can be observed at the capacitance signals, and therefore results in a non-stable value of capacitance ratio. To alleviate this problem, an algorithm using RLS method enhanced by adaptive forgetting factors is developed.

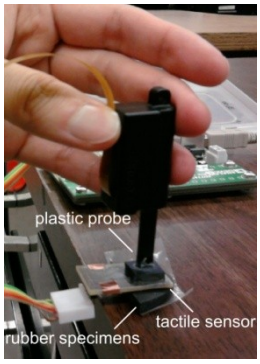

Fig. 5. Tactile sensor pushing against rubber specimens in a handheld mode.

TABLE I YOUNG'S MODULI OF THE SORBOTHANE RUBBER SPECIMENS FOR THE SENSOR TESTS

Shore scale	Young's Modulus (MPa)
30 OO	0.143
40 OO	0.186
50 OO	0.289
60 OO	0.405
70 OO	0.515
30 A	0.87
40 A	1.54
50 A	2.18
60 A	3.46
70 A	8.68

A. Recursive Least-Squares (RLS) Identification

The capacitance readouts can be formulated in an identification form shown in (3).

$$C_1(k) = C_2^T(k) r_c(k) + e(k) \tag{3}$$

where $C_1(k)$ and $C_2(k)$ represent the capacitance values which can be viewed as the output and input data for an dynamic identification model. It can also be seen that $r_c(k)$ serves as the estimated parameter, while $e(k)$ is the identification error.

By implementing a RLS algorithm[8-10], the unknown parameter $r_c(k)$ can be iteratively updated at each sampling time. Through this process, the sum of estimation errors can be minimized. The procedure of identifying the capacitance ratio can be described in the following steps.

Step 1: Read the sensor readouts, $C_1(k)$ and $C_2(k)$.

Step 2: Calculate the identification error, $e(k)$, which is the difference between $C_1(k)$ at this sample and the estimated $C_1(k)$, which is the product of $C_2(k)$ and the estimated ratio in previous sample $r_c(k-1)$, i.e.

$$e(k) = C_1(k) - C_2^T(k) r_c(k-1) \tag{4}$$

Step 3: Calculate the update gain vector, $K(k)$, as

$$K(k) = \frac{P(k-1)C_2(k)}{\lambda + C_2^T(k)P(k-1)C_2(k)} \tag{5}$$

and calculate the covariance matrix, $P(k)$, using

$$P(k) = \frac{1}{\lambda}\left[P(k-1) - \frac{P(k-1)C_2(k)C_2^T(k)P(k-1)}{\lambda + C_2^T(k)P(k-1)C_2(k)} \right] \tag{6}$$

Step 4: Update the estimated parameter, $r_c(k)$, as

$$r_c(k) = r_c(k-1) - K(k)e(k) \tag{7}$$

The parameter, λ, in the above equations is known as the forgetting factor. By properly adjusting λ, the influence of old data, which may no longer be relevant to the model, can be suppressed. The use of the forgetting factor not only prevents a covariance wind-up problem, but also allows a fast tracking of the changes in process. A typical value of the forgetting factor is suggested to be in the interval 0.9 to 1 [8]. It can also be intuitively understood that the RLS algorithm utilizes a batch of $N = 2/(1-\lambda)$ samples to update the current estimation. When $\lambda = 1$, all the previous data collected will be used. A smaller λ value usually results in a faster convergence of estimates. However, a reduced value of λ increases the sensitivity of estimation to measurement noise, which may cause oscillatory estimation. Therefore a tradeoff between the fast-tracking capability and high immunity to noise should be considered in the system design, which will be addressed next.

B. Fast Convergence Rate versus Immunity to Noise

To illustrate how the size of the forgetting factor can influence the performance of the ordinary RLS algorithm, the estimation is conducted during sensor touch on two rubber samples, 30OO and 30A, respectively, as shown in Fig. 6.

As can be seen, with a relatively large forgetting factor ($\lambda = 0.995$), the estimation of parameter is considerably stable without observable oscillations after it converges, which is appealing for good parameter estimation. On the other hand, a smaller forgetting factor ($\lambda=0.9$) results in a faster convergence at the cost of larger oscillations at steady state.

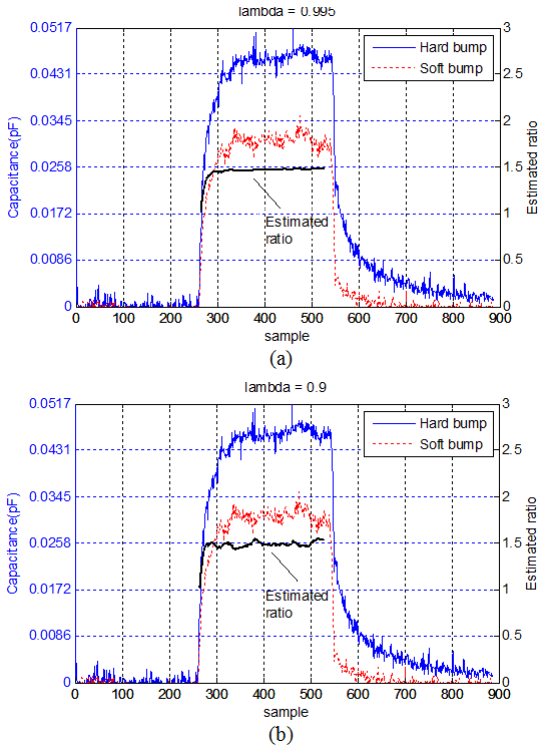

Fig. 6. Sensor readouts on sample 30OO, estimation using ordinary RLS : (a) $\lambda = 0.995$ (b) $\lambda = 0.9$.

C. *RLS with Adaptive Forgetting Factors*

As discussed in the previous sub-section, it would be beneficial to implement an adaptive algorithm for the forgetting factor to achieve both the favorable properties of fast-tracking and immunity to measurement noise. Hence a change detection algorithm is necessary to differentiate between transient states and the steady state. For instance, in [8], a change detection algorithm was used to detect the abrupt change of friction coefficient between the automobile tire and a snow covered road. This algorithm was used to trigger the amplification of the covariance matrix (gain matrix) to adaptively control the convergence rate. Similarly, in our case, a change detection of capacitance ratio would facilitate the adjustment of forgetting factors. The CUSUM [11, 12] change detection algorithm is chosen for its simplicity. The identification error *e(k)* is monitored throughout the period of contact. An alarm is signaled if the identification error has been larger than a threshold for a certain amount of time. The recursive formula of this method is shown below.

$$a_k = \max(a_{k-1} + |e_k| - d, 0), \quad k = 1,2,... \qquad (8)$$
$$a_0 = 0$$

As can be seen, given the identification error e_k calculated in an ordinary RLS as the input, an output alarm signal can be generated. If the alarm value $a_k > h$, a smaller forgetting factor will be chosen in the RLS. Here, the threshold value h is used to determine when the forgetting factor should be adjusted in the condition that for how long an alarm signal has been on. The other threshold value d in the above equation is used to judge when to turn on the alarm. This makes the process ignore errors smaller than d. If the estimation system can swiftly track any abrupt change in capacitance ratio, the identification error will drop below a certain level, thus resulting in a zero value of the alarm signal. At this stage, the alarm is turned back off and a larger forgetting factor is chosen for its high immunity to noise at a steady-state.

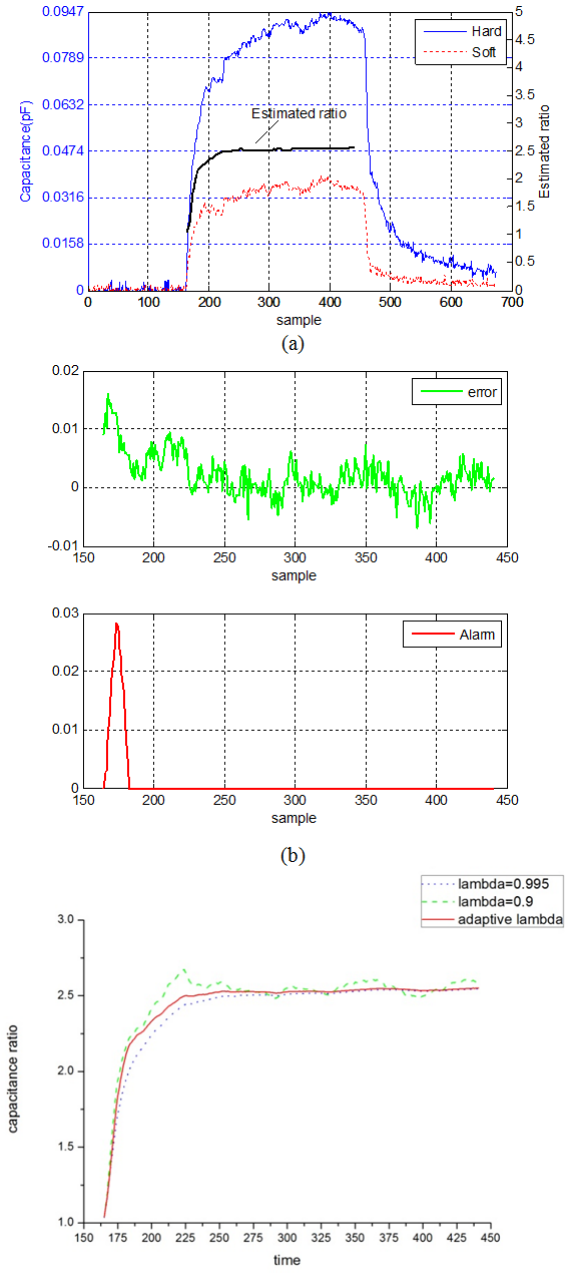

Fig. 7. Sensor readouts on sample 70OO: (a) esimation of capacitance ratio using RLS with adaptive forgetting factors (b) identification error and alarm signal (c) comparison of estimation results of ordinary RLS with $\lambda = 0.995$, $\lambda = 0.9$, and adaptive forgetting factors.

To demonstrate this algorithm, an experimental test on touching sample 70OO is conducted and the results are

illustrated in Fig. 7. As shown in Fig. 7(a), capacitance values of the hard and soft elements are plotted and the estimation is performed by using RLS with adaptive forgetting factors. It can be seen that contact occurs at around the 150th sample, where the estimation starts. At the beginning the estimation error is larger than 0.01, which triggered the alarm signal [Fig. 7(b)]. When the alarm signal is on for a while, a relatively small forgetting factor (λ=0.9) is chosen. After the identification error drops to a certain level, the alarm signal is turned off, and a larger forgetting factor (λ=0.995) is then applied throughout the rest of estimation process. To illustrate the benefit of this adaptive algorithm, estimation results of ordinary RLS with $\lambda = 0.995$, $\lambda = 0.9$, and adaptive forgetting factors are shown in Fig. 7(c). As shown in the figure, the etimation results generated by λ=0.9 show the favarable propety of fast-tracking of changes. However, it is susceptible to measurement noise, which makes it difficult to identify the true value of the capacitance ratio. The alogrithm of using adaptive forgetting factor inherits the desirable property of fast convergence to a true value at the beginning stage, and then trends to the curve of λ=0.995, which holds a relatively constant value at the steady state.

D. Estimations on Multiple Rubber Samples by Utilizing RLS with Adaptive Forgetting Factors

To further demonstrate the performance of the estimation system, experimental tests of touching multiple rubber samples consecutively one by one are performed. As shown in Fig. 8, rubber sample 30OO, 70OO, 40A and 70A are touched consecutively by the tactile sensor.

The test results are shown in Fig. 9. A real-time estimation of capacitance ratio can be generated by using the developed algorithm. For each touch, 250 samples of the data are utilized for the estimation right after the contact, so that the same estimation time can be applied for all the tests. When the estimation is completed, the capacitance ratio is then set back to one to maintain the same initial value for all the estimations. As can be seen, the estimated ratio increases as the sample under contact becomes harder. The size of alarm signal also grows larger for harder samples, which is likely due to the larger initial identification error when touching harder samples.

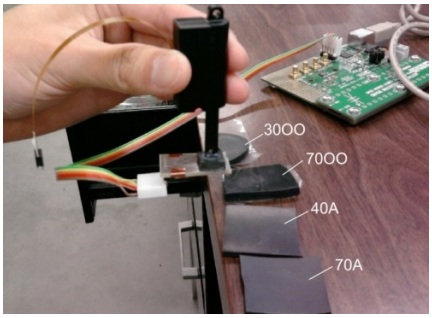

Fig. 8. Push the tactile sensor towards four rubber specimens on by one

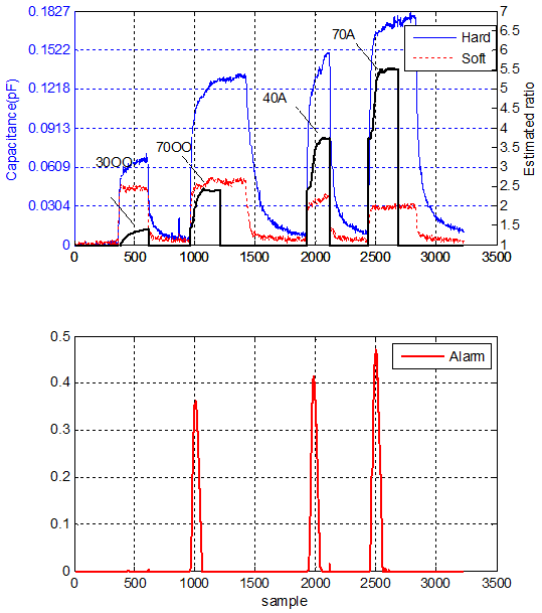

Fig. 9. Sensor readouts, estimation of capacitance ratio, and alarm signal during the test on four different samples (30OO, 70OO, 40A and 70A, from soft to hard).

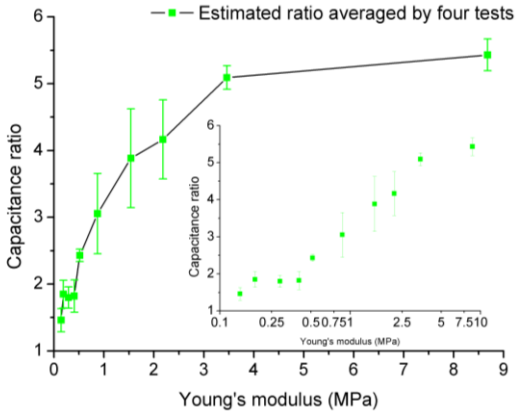

Fig. 10. Estimated capacitance ratio versus Young's modulus of the rubber sample. Inserts: data plotted in lin-log scale.

IV. Characterization of Tactile Sensor Using Rubber Specimens

With the developed estimation algorithm, the tactile sensor is characterized by touching a variety of rubber specimens. Each rubber sample has been touched four times and the estimated capacitance ratio for each test has been recorded. As shown in Fig. 10, the capacitance ratio shows an overall uptrend as the rubber sample becomes harder. It can also be observed that some measurements have a considerable amount of standard deviation as depicted by error bars on the plot. This variation is likely due to oblique contact between the sensor and rubber samples as well as the nonlinearity of the capacitance response to the applied load on the bump, which cannot be solved solely by using the developed estimation algorithm. Our tests also show that these variations can be significantly reduced by mounting the sensor on a test stage and applying constant loads throughout all the tests. However, this stage test is not within the scope of this paper,

since this paper focuses on developing estimation algorithms for a handheld device.

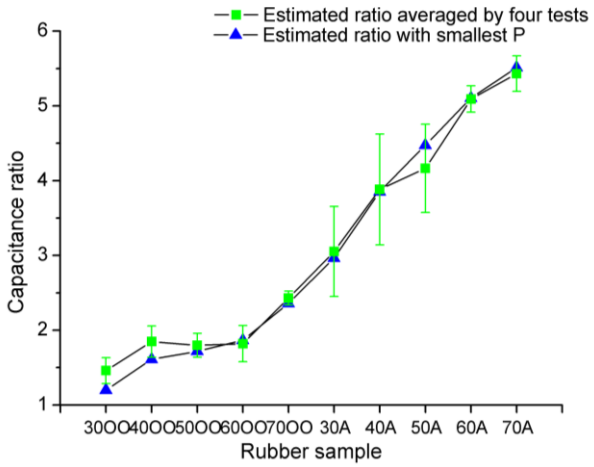

Fig. 11. Estimated capacitance ratio for all the rubber samples.

Although the variation in measurement of a handheld tactile sensor cannot be completely eliminated by using the developed estimation algorithm, the estimation system also provides a quantitative criterion to determine the reliability of the estimated value. In other words, the estimation system can also be used to verify which test provides a more reliable value of the capacitance ratio. This decision can be accomplished by comparing the covariance (P) of the estimation among several tests. It is likely that a smaller covariance will represent a more reliable estimation. The estimated ratios with the smallest covariance for each set of data are plotted in Fig. 11, to compare with the averaged value obtained from all four tests. This plot shows a precise uptrend, which coincides with the increase of elasticity of the rubber samples. Finally, the relation between the Young's moduli of the rubber samples and sensor measurements (capacitance ratio) is plotted on Fig. 12. A curve derived from (2) is used to fit the measurements. The estimated parameters coincide well with the sensor design.

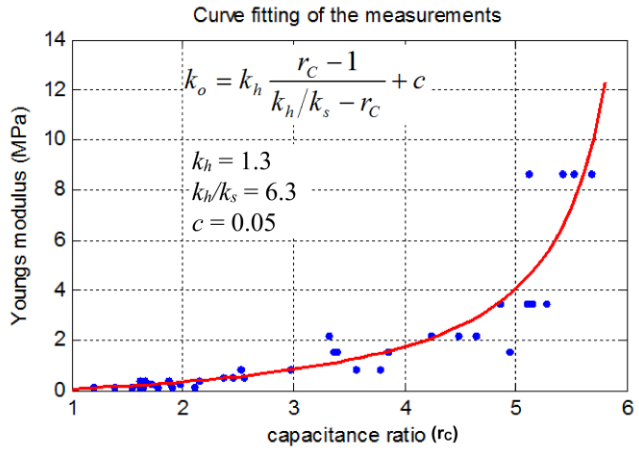

Fig. 12. Curve fitting for Young's moduli of rubber specimens vs. sensor measurements.

V. Conclusion

This paper presented an estimation algorithm to identify the capacitance ratio from readouts of a novel tactile sensor for elasticity measurement. This estimation algorithm utilizes the recursive least-squares method enhanced by an adaptive forgetting factor algorithm. By using this algorithm, the true value of the capacitance ratio not only can be swiftly tracked, but also shows high immunity to measurement noise at the steady state. This algorithm has been successfully applied in the presented tactile sensor and could also be employed by other handheld devices to alleviate the noise caused by hand vibration. Finally, the characterization of the tactile sensor indicates that the covariance of the estimation can serve as a quantitative reference for choosing a reliable measurement among a set of tests.

Acknowledgment

Financial support for this research was partly provided by the Minimally Invasive Medical Technologies Center (MIMTeC, www.mimtec.org), a National Science Foundation – Industry – University Cooperative Research Center. Sensor fabrication was performed at the Nano-fabrication Center at the University of Minnesota which is supported by the NSF's National Nanotechnology Infrastructure Network (NNIN).

References

[1] J. Tegin and J. Wikander, "Tactile sensing in intelligent robotic manipulation - a review," *Industrial Robot-an International Journal,* vol. 32, pp. 64-70, 2005.

[2] R. Aoyagi and T. Yoshida, "Frequency equations of an ultrasonic vibrator for the elastic sensor using a contact impedance method," *Japanese Journal of Applied Physics Part 1-Regular Papers Short Notes & Review Papers,* vol. 43, pp. 3204-3209, May 2004.

[3] Y. Murayama, *et al.*, "Development of a new instrument for examination of stiffness in the breast using haptic sensor technology," *Sensors and Actuators a-Physical,* vol. 143, pp. 430-438, May 16 2008.

[4] G. Tholey, *et al.*, "Force feedback plays a significant role in minimally invasive surgery - Results and analysis," *Annals of Surgery,* vol. 241, pp. 102-109, Jan 2005.

[5] P. Peng, *et al.*, "Novel MEMS stiffness sensor for in-vivo tissue characterization measurement," *Proceedings of IEEE Engineering in Medicine Biology Society,* vol. 1, pp. 6640-6643, 2009.

[6] P. Peng, *et al.*, "Novel MEMS stiffness sensor for force and elasticity measurements," *Sensors and actuators. A, Physical,* vol. 158, pp. 10-17, 2010.

[7] P. Peng, *et al.*, "Flexible Tactile Sensor for Tissue Elasticity Measurements," *Journal of microelectromechanical systems,* vol. 18, pp. 1226-1233, 2009.

[8] J. Wang, *et al.*, "Friction estimation on highway vehicles using longitudinal measurements," *Journal of dynamic systems, measurement, and control,* vol. 126, p. 265, 2004.

[9] S. Sastry and M. Bodson, *Adaptive control: stability, convergence, and robustness*, 1989.

[10] F. Gustafsson, *Adaptive filtering and change detection*: Wiley Londres, 2001.

[11] E. Page, "Continuous inspection schemes," *Biometrika,* vol. 41, p. 100, 1954.

[12] R. Rajamani, "Radar health monitoring for highway vehicle applications," *Vehicle System Dynamics,* vol. 38, pp. 23-54, 2002.